

Supporting Information for:

## **A Reproducible Mechano-responsive Luminescent System Based on Discotic Crown Ether Derivative Doped with Fluorophore: Taking Advantage of the Phase Transition of Matrix**

*Ben Zhang,<sup>a</sup> Chih-Hao Hsu,<sup>b</sup> Zhen-Qiang Yu,<sup>c</sup> Shuang Yang,<sup>a</sup> and Er-Qiang Chen<sup>a\*</sup>*

<sup>a</sup> *Beijing National Laboratory for Molecular Sciences, Key Laboratory of Polymer Chemistry and Physics of the Ministry of Education, College of Chemistry and Molecular Engineering, Peking University, Beijing 100871, China*

<sup>b</sup> *Department of Polymer Science, College of Polymer Science and Polymer Engineering, The University of Akron, Akron, Ohio, 44325-3909, USA*

<sup>c</sup> *School of Chemistry and Chemical Engineering, Shenzhen Key Laboratory of Functional Polymers, Shenzhen University, Shenzhen 518060, China*

### **General Methods and Materials**

All reagents and solvents were purchase from Beijing Chemical Reagent Company. Tetrahydrofuran (THF) were refluxed over CaH<sub>2</sub> and distilled before use. Pyridine was dry by MgSO<sub>4</sub> for 48 h and then distilled before use.

<sup>1</sup>H NMR and <sup>13</sup>C NMR spectra were recorded on a Bruker ARX400 spectrometer in CDCl<sub>3</sub> solutions (400 and 100 MHz for <sup>1</sup>H NMR and <sup>13</sup>C NMR, respectively). Chemical shifts of <sup>1</sup>H and <sup>13</sup>C NMR were quoted to internal standard Me<sub>4</sub>Si. Mass spectra were recorded on a Bruker Autoflex III MALDI-TOF. Elemental analyses were carried out with an Elementar Analysensysteme GmbH vario EL Elemental Analyzer.

Differential scanning calorimetry (DSC) measurements were carried out on a DSC Q100 (TA Instruments). A typical mass of ~1 mg sample was encapsulated in a sealed aluminum pan with the pan weight identically matched to the reference pan.

One-dimensional (1D) powder X-ray diffraction (XRD) experiments were performed on a Philips X'Pert Pro diffractometer with a 3 kW ceramic tube as the X-ray source (Cu K $\alpha$ ) and an

X'celerator detector. The 1D XRD was also performed with a SAXSess (Anton Paar) equipped with Kratky block-collimation system. The scattering pattern was recorded on an imaging plate (IP) with a pixel size of  $42.3 \times 42.3 \mu\text{m}^2$  which extended to the high-angle range (the  $q$  range covered by the IP was from 0.06 to  $29 \text{ nm}^{-1}$ ). Background subtraction and desmearing were conducted by using SAXSquant 3.6 software. For the sheared samples with the shear direction aligned parallel to the line-focused X-ray incident beam of SAXSess, desmearing of the scattering intensity was not further performed. Two-dimensional (2D) XRD experiments were performed on a Bruker D8Discover diffractometer with a 3 kW ceramic tube as the X-ray source ( $\text{Cu K}\alpha$ ) and a GADDS as the 2D detector. For the XRD experiments, the reflection peak positions were calibrated with silicon powder ( $2\theta > 15^\circ$ ) and silver behenate ( $2\theta < 10^\circ$ ).

Transmission electron microscopy (TEM) experiments were conducted using Philips Tecnai 12 at an accelerating voltage of 120 kV. The sample for electron diffraction (ED) was prepared by vigorous mechanical shear on molecule **1** on the carbon-coated mica at  $70^\circ\text{C}$  followed by quenching to room temperature. The sample on the carbon film was then floated on the water surface and picked up by a TEM copper grid (300 mesh, SPI). Before TEM and ED experiments, samples were put into a vacuum chamber for 12 hours to remove the residual moisture.

Polarized optical microscopy (POM) images were recorded using a Leica DLMP microscope. The sample was placed on a glass slide. Fluorescent microscopic images were taken on A1R-siLaser Scanning Confocal Microscope, irradiation at 405 nm and emission through the 515/30 nm filter.

Ultraviolet-visible (UV-vis) absorption was recorded using a Hitachi U-410 UV-vis spectrometer and the samples were placed on quartz plates. Fluorescent spectra were detected using FLS920 fluorescence spectrometer.

Rheological experiment was carried out on ARES-G2rheometer with 8 mm diameter parallel-plate geometry. The sample thickness is 0.66 mm and the shear rate is  $10 \text{ s}^{-1}$ .

## Computer Simulation

The molecular modeling of molecule **1** was conducted on the Accelrys Cerius<sup>2</sup> package with COMPASS force field for energy minimization. To build the crystal unit cell, the lattice dimensions were extracted from the analysis of XRD data, and the space group  $P1$  was chosen

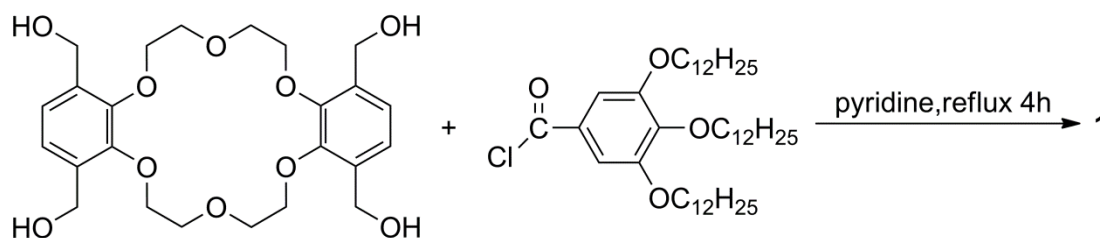
preliminarily. The peripheral C12 alkyl tails on molecule **1** was truncated to C6 to simplify the complex conformation of long alkyl tails in the simulated result, yet reserve the conformational restriction for the alkyl repeat units closed to the core of molecule **1**. The rest C6s are evenly spaced in the unit cell to make the electron density reasonable throughout the unit cell. The arrangement of molecules in the unit cell was mainly generated via energy minimization followed by minor modifications to simulate the best fit to the experimental XRD data.

### Preparation of mixture 1/DETPTS:

**DETPTS** was synthesized according to literature procedures.<sup>[1]</sup> To prepare the mixture of **1** and **DETPTS**, the two compounds were dissolved in the solvent of THF with a molar ratio of 20:1 followed by evaporating the solvent. The resulted solid was well-mixed by heating to 180 °C, where is beneath the decomposed temperatures of **1** and **DETPTS**. The mixture did not take macrophase separation at temperatures above the isotropic temperature of **1**. After **1** formed LC phases at low temperatures, **DETPTS** dispersed well in the mixture (see Figure S14).

### Synthesis and Characterization of the Crown Ether Derivative **1**

3,3',6,6'-tetrakis(hydroxymethyl)dibenzo-18-crown-6<sup>[2]</sup> and 3,4,5-tri(*n*-dodecyloxy)benzoyl chloride<sup>[3]</sup> were prepared following the literature procedures. Molecules **1** was synthesized followed the synthetic route shown in Scheme S1.



**Scheme S1.** Synthetic route of crown ether derivatives **1**.

### 3,3',6,6'-tetrakis[3'',4'',5''-tri(*n*-dodecyloxy)benzoxymethyl]dibenzo-18-crown-6 (**1**)

3,3',6,6'-tetrakis(hydroxymethyl)dibenzo-18-crown-6 (60 mg, 0.12 mmol), 3,4,5-tri(*n*-dodecyloxy)benzoyl chloride (347 mg, 0.50 mmol) were dissolved in 20 mL dry pyridine. The mixture was then refluxed for 4 h and then cooled to room temperature (RT). The solution was filtered, and then solvent was evaporated under reduced pressure. The residue was purified by chromatography on silica gel (eluent: petroleum ether/ dichloromethane/ ethyl acetate =2: 2: 0.5) to

afford 320 mg **1** (yield: 83%) as white solid.  $^1\text{H}$  NMR (400MHz,  $\text{CDCl}_3$ ):  $\delta$  = 0.85 (t, 36H,  $\text{CH}_3$ ), 1.25 (m, 192H,  $\text{CH}_2$ ), 1.48 (m, 24H,  $\text{CH}_2$ ), 1.78 (m, 24H,  $\text{CH}_2$ ), 3.96 (m, 32H,  $\text{OCH}_2$ ), 4.32 (m, 8H,  $\text{OCH}_2$ ), 5.41 (s, 8H,  $\text{OCH}_2$ ), 7.19 (s, 4H, ArH).  $^{13}\text{C}$  NMR (100 MHz,  $\text{CDCl}_3$ ):  $\delta$  = 14.12, 22.71, 26.08, 26.14, 29.36, 29.38, 29.40, 29.44, 29.60, 29.66, 29.67, 29.71, 29.75, 30.37, 31.94, 61.72, 69.26, 70.73, 72.68, 73.54, 108.14, 124.49, 124.65, 131.05, 142.69, 150.57, 152.91, 166.22. Elemental analysis (%) calcd. for  $\text{C}_{196}\text{H}_{336}\text{O}_{26}$ : C75.72; H10.89; Found: C75.51; H11.00. MS (MALDI-TOF):  $m/z$  3129.9 (calcd. $[\text{M}+\text{Na}-1]^+=3130.5$ ).

### Figures and Table:

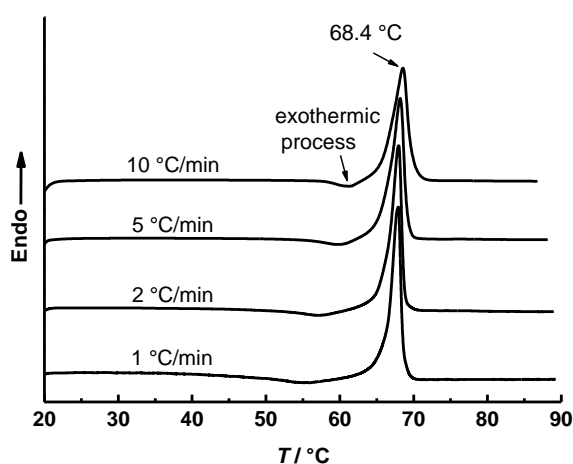


**Figure S1.** DSC heating traces of the quenched sample ( $\text{Col}_h$  phase) of **1** recorded at various heating rates. Note that there is a broad exothermic process before the isotropization temperature around 68 °C. According to the temperature dependent XRD result (Figure 2b in the manuscript), the exothermic process associates with the  $\text{Col}_h$  to  $\text{LC}_x$  transition. As shown by the DSC data, the slower the heating rate, the lower temperature at which the  $\text{Col}_h$ -to- $\text{LC}_x$  transition starts. This behavior is similar to a Cr-Cr phase transition upon slowly heating that found in the discotic triphenylene derivative.<sup>[4]</sup> For the limited experimental conditions, we were unable to monitor the thermal behavior of the formation of  $\text{Col}_h$  upon rapid cooling from melt.

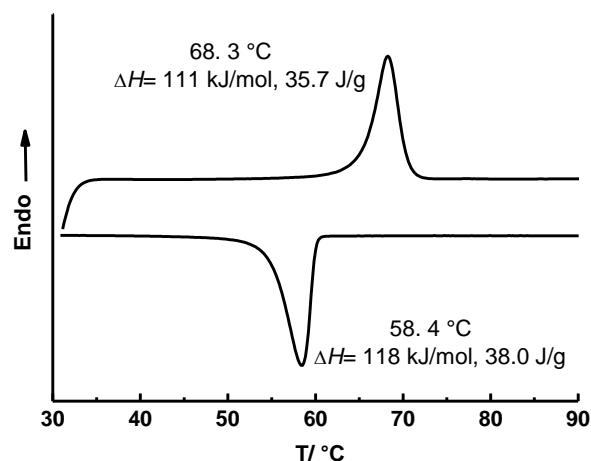


**Figure S2.** DSC traces of **1** recorded upon cooling and subsequent heating at a normal rate of  $10\text{ °C min}^{-1}$ . Note that the  $\Delta H$  of the transitions into and out of the  $\text{LC}_x$  phase is pretty large. A possible explanation for this may be that the oxygen rich structure of molecule **1** with a large mole mass of  $3108\text{ g mol}^{-1}$  enhances the intermolecular interactions. Large enthalpies of transitions from crystalline phase into LC ( $\text{Col}_h$  or cubic) phases were found in high molecular weight dendrons.<sup>[5]</sup>

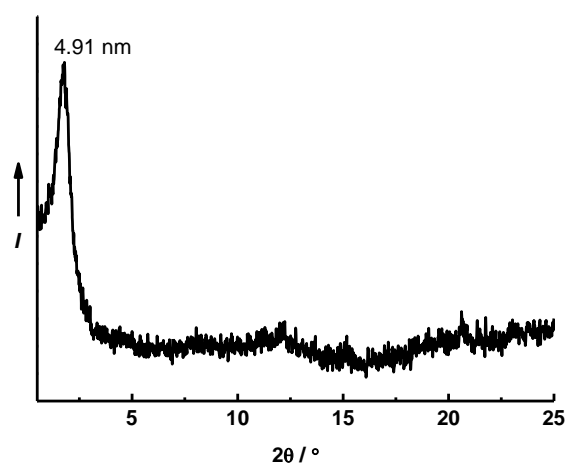


**Figure S3.** XRD pattern of **1** after it was cooled from melt to room temperature (RT) at a rate of  $2\text{ °C min}^{-1}$ .



**Figure S4.** The original POM picture of **1** under crossed polarizers recorded upon cooling to RT from melt at a rate of  $2\text{ }^{\circ}\text{C min}^{-1}$ .

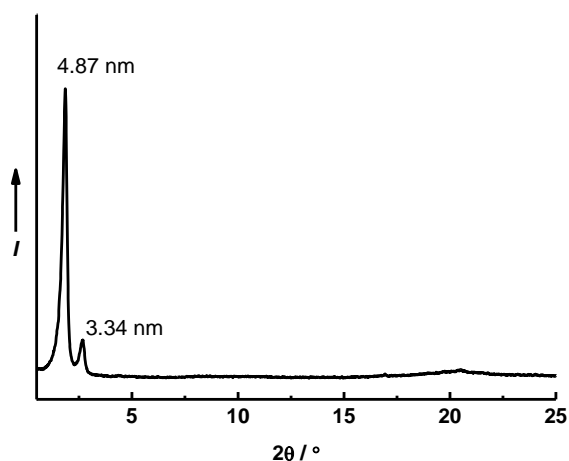


**Figure S5.** XRD pattern of **1** recorded at RT. The sample was first cooled from its melt to  $60\text{ }^{\circ}\text{C}$  followed by isothermal annealing for 48 h, and then further cooled to RT.

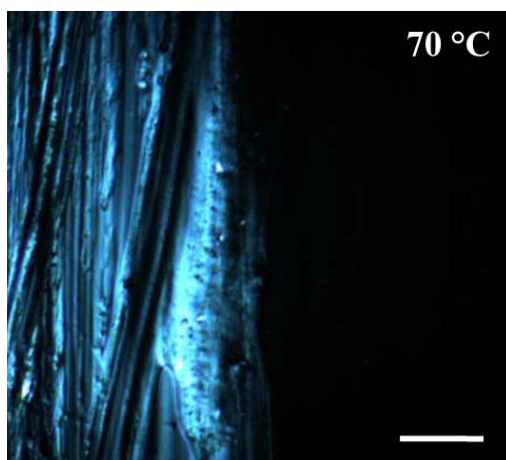


**Figure S6.** POM image of **1** under crossed polarizers at  $70\text{ }^{\circ}\text{C}$ . The left part was subjected to shear, while the right part was undisturbed. Scale bar:  $500\text{ }\mu\text{m}$ .

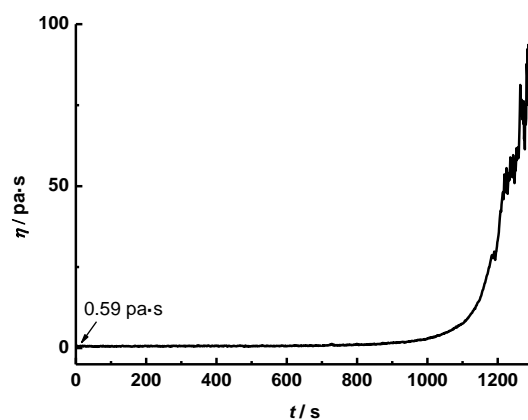


**Figure S7.** The rheological experiment of compound **1** measured at  $70\text{ }^\circ\text{C}$ . As the Cr phase growing, the sample was expelled from the plates visibly at the time around 1050 s and the irregular data was observed afterwards.

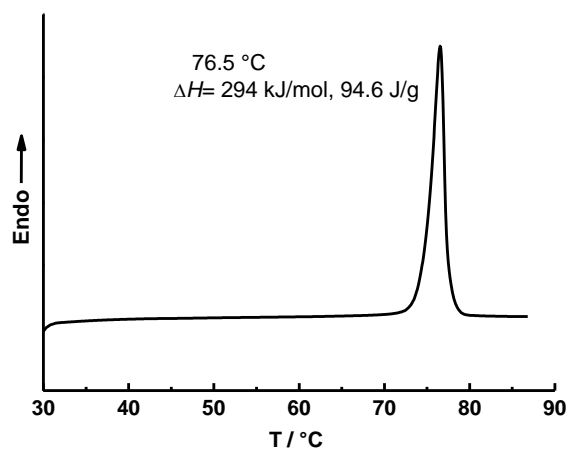


**Figure S8.** DSC trace of **1** recorded after it was sheared at  $70\text{ }^\circ\text{C}$  followed by cooling to RT. The heating rate was  $10\text{ }^\circ\text{C min}^{-1}$ .

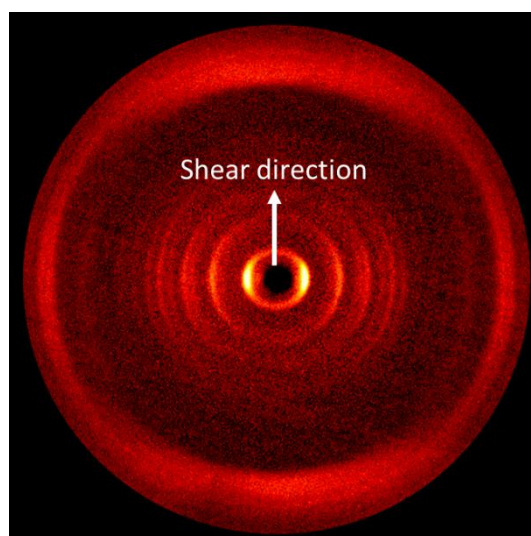


**Figure S9.** 2D XRD pattern of **1** in the Cr phase oriented by mechanical shearing. The shear direction is along the meridian.

**Table S1. Diffractions of the crystalline orthorhombic phase**

<i>hkl</i>	100	010	200	020	210	120	220	310	030	130
$d_{\text{exp}}^{\text{a}}/\text{nm}$	3.41	3.05	1.70	1.53	1.52	1.41	1.13	1.08	1.02	0.98
$d_{\text{cal}}^{\text{b}}/\text{nm}$	3.41	3.05	1.71	1.53	1.49	1.39	1.14	1.07	1.02	0.97
<i>hkl</i>	320	230	400	040	330	240	430	250	440	350
$d_{\text{exp}}/\text{nm}$	0.94	0.86	0.85	0.78	0.77	0.71	0.65	0.58	0.57	0.54
$d_{\text{cal}}/\text{nm}$	0.91	0.87	0.85	0.76	0.76	0.70	0.65	0.57	0.57	0.54
<i>hkl</i>	710	001	360	021	730	270	041	280		
$d_{\text{exp}}/\text{nm}$	0.48	0.47	0.46	0.45	0.44	0.42	0.40	0.37		
$d_{\text{cal}}/\text{nm}$	0.48	0.47	0.46	0.45	0.44	0.42	0.40	0.37		

<sup>a</sup> experimental value. <sup>b</sup> calculated value based on  $a = 3.41$  nm,  $b = 3.05$  nm and  $c = 0.47$  nm.



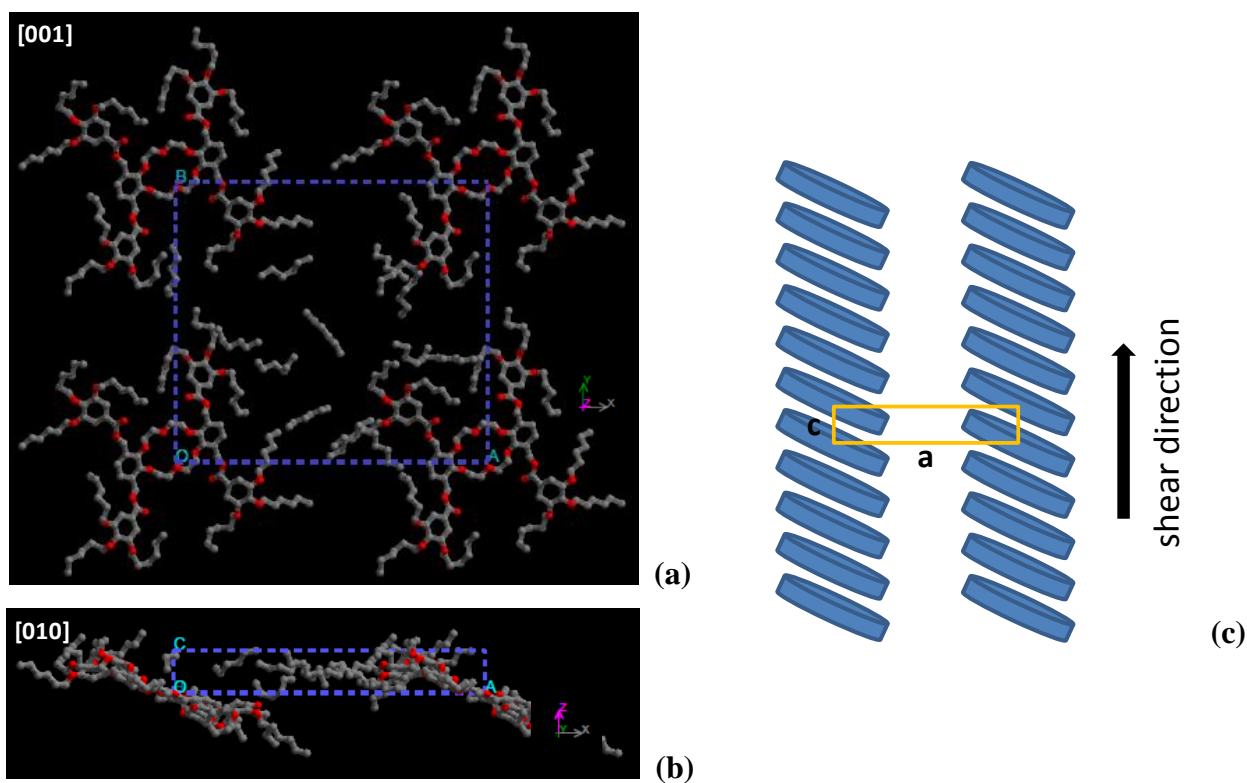


**Figure S10.** Molecular packing scheme simulated by Cerius<sup>2</sup>. The orthorhombic unit cell possesses the dimensions of  $a = 3.41$  nm,  $b = 3.05$  nm, and  $c = 0.47$  nm. To perform the simulation effectively yet keep the model close to the real **1**, the C12 alkyl tail was truncated to C6. Moreover, to make the electron density reasonable throughout the unit cell determined by the experiments, the rest C6s were evenly placed in the unit cell. (a) and (b) the view of molecular packing along the  $c$ - and  $b$ -axis, respectively. (c) Schematic draw of the molecular packing obtained by shearing.

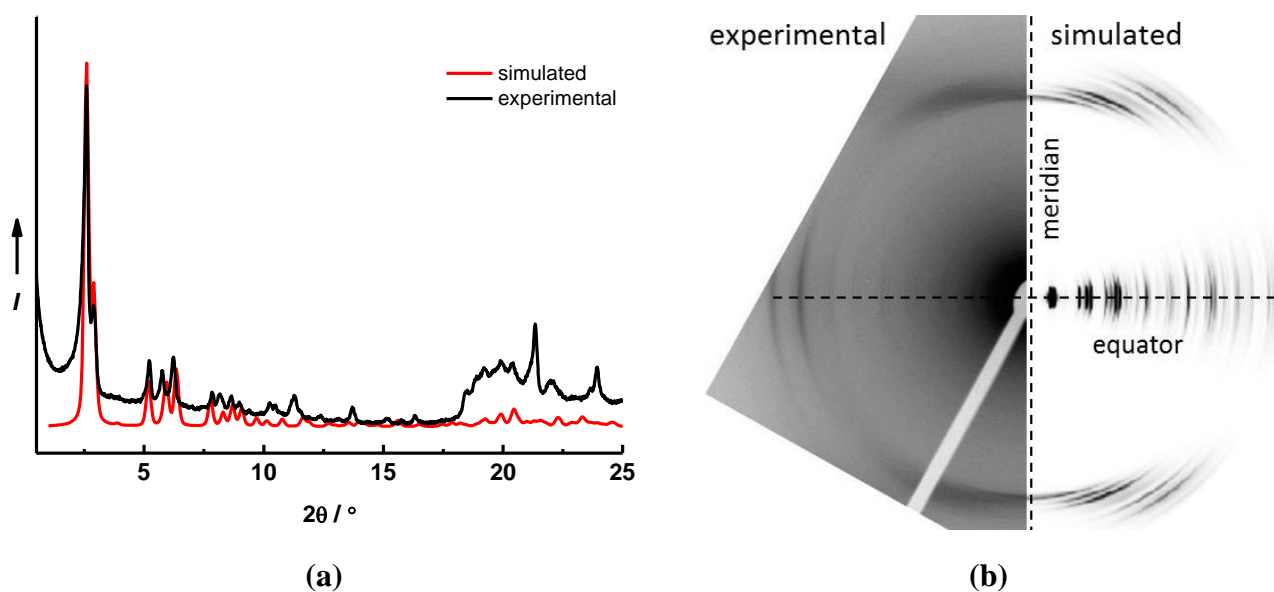


**Figure S11.** Comparison between the simulated diffraction based on the packing model shown in Figure 3d and Figure S9 and the experimental data. (a) 1D XRD profile; (b) ED pattern.

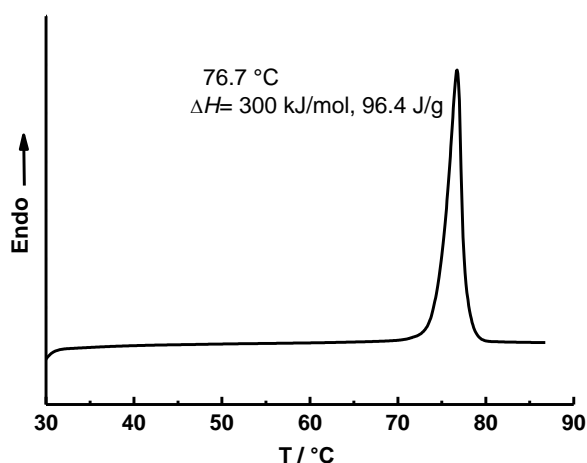


**Figure S12.** DSC heating trace of **1** after sheared at 60 °C. The initial sample was in the LC<sub>x</sub>. After sheared at 60 °C, it was transformed into Cr phase. The heating rate was 10 °C min<sup>-1</sup>.

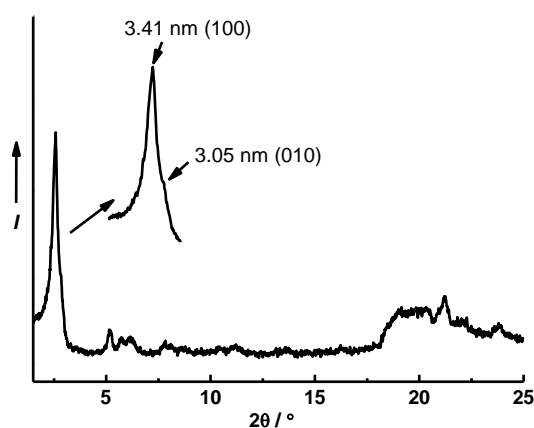


**Figure S13.** XRD pattern recorded at RT of **1** after sheared at 60 °C. The initial sample was in the LC<sub>x</sub>. After sheared at 60 °C, it was transformed into Cr phase.

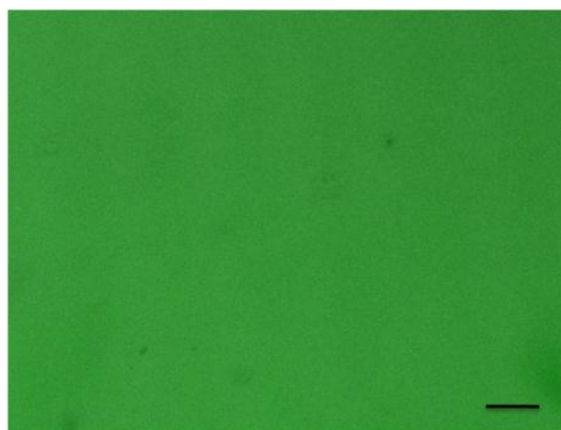


**Figure S14.** Confocal fluorescence microscopic image of the mixture **1**/DETTPS (molar ratio of 20:1) at RT. Scale bar: 10 μm.

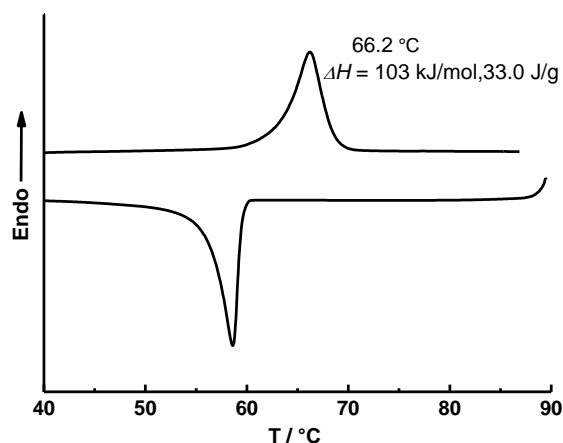


**Figure S15.** DSC traces of mixture 1/DETIPS (molar ratio of 20:1) recorded upon cooling and subsequent heating at a rate of  $10^\circ\text{C min}^{-1}$ .

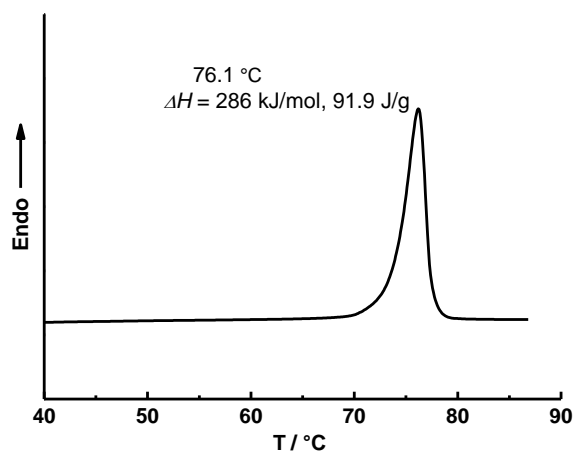


**Figure S16.** DSC heating trace of mixture 1/DETIPS (molar ratio of 20:1) recorded after the mixture was sheared at  $70^\circ\text{C}$  followed by cooling to RT. The heating rate was  $10^\circ\text{C min}^{-1}$ .

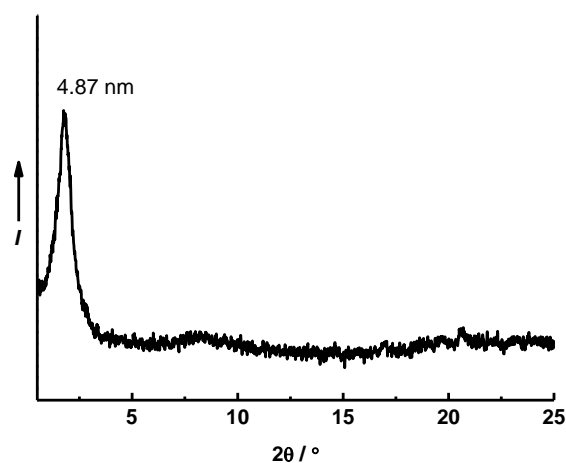


**Figure S17.** XRD pattern of mixture 1/DETIPS (molar ratio of 20:1) cooled from melt to RT at a rate of  $2^\circ\text{C min}^{-1}$ .

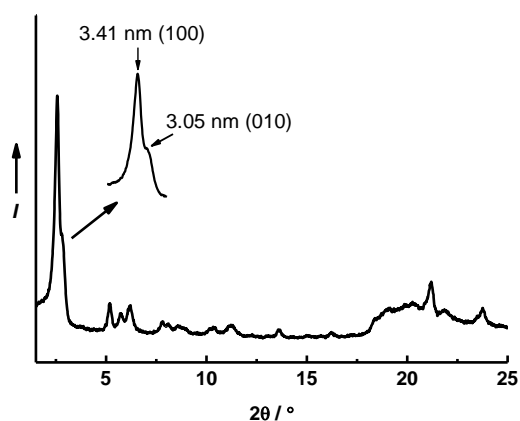


**Figure S18.** XRD pattern of mixture **1/DETIPS** (molar ratio of 20:1) after sheared at 70 °C.

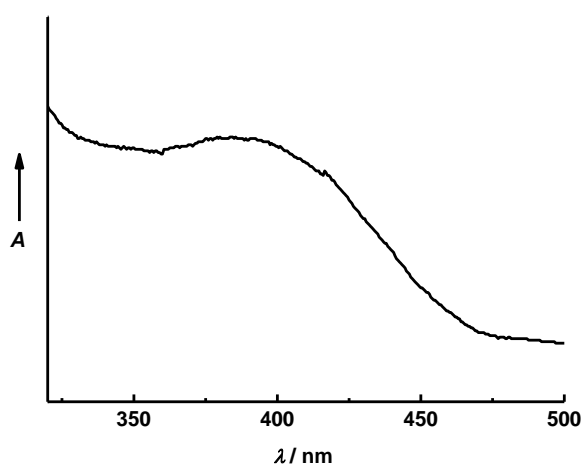


**Figure S19.** Absorption spectrum of **1/DETIPS** (molar ratio of 20:1) in the LC<sub>x</sub> phase recorded at RT.

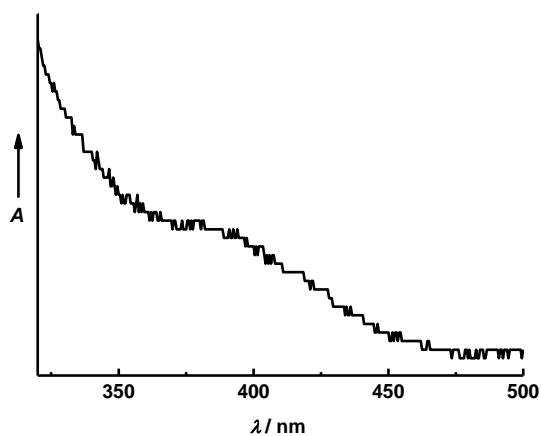


**Figure S20.** Absorption spectrum of **1/DETIPS** (molar ratio of 20:1) in the Cr phase recorded at RT.

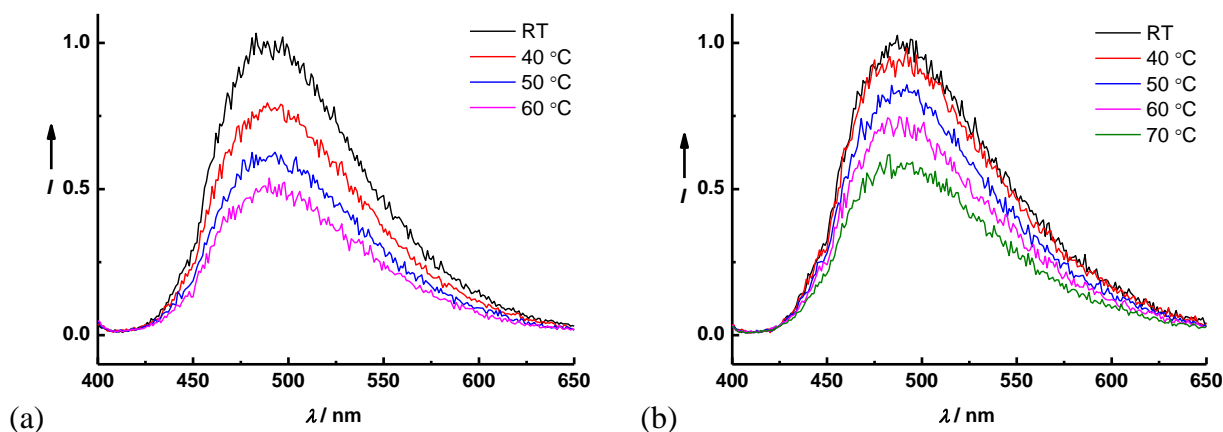


**Figure S21.** Normalized emission spectra recorded on heating of **1/DETPS** (molar ratio of 20:1) in the LC<sub>x</sub> phase (a) and in the Cr phase (b). In both cases,  $\lambda_{\text{ex}} = 380$  nm.

We checked the fluorescence of **DETPS** in **1** with different phases again, of which the results indicated that both the wavelengths were not significantly affected by the phase transitions, as shown in Figure S21. The samples in both LC<sub>x</sub> and Cr phase give the emission with the similar fluorescence wavelength. The absorption (Fig. S19 and S20) and fluorescence wavelengths are not influenced apparently by the change of surrounding of dye molecules. The similar phenomena was reported in the literature. For example, for 9-(2-carboxy-2-cyanovinyl)julolidine (**CCVJ**) in ethylene glycol/glycerol mixture, when the amount of glycerol increased, the viscosity of the mixture increased, leading to enhanced emission intensity of **CCVJ**, while fluorescence wavelength kept the same.<sup>[6]</sup> For hexaphenylsilole (**HPS**), which has a similar chemical structure to **DETPS**, enhanced emission intensity was detected when aggregation was formed by adding water to its acetone solution. But the absorption and fluorescence wavelength are almost unchanged.<sup>[1]</sup> We speculate that the molecular conformation and the energy gap between the ground and excited states of **DETPS** dye molecule may not be much affected in different phases of compound **1**.

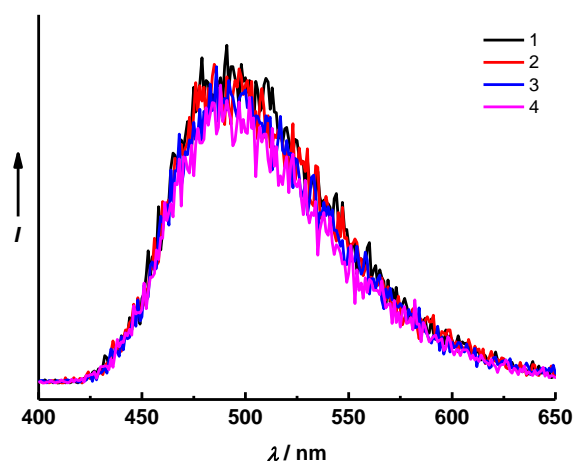


**Figure S22.** Fluorescent spectra of the shear-induced phase upon four repeating cycles. During each cycle, the sample was first heated to the melt state (80 °C), scratched at 70 °C, cooled down to RT, and then heated to 80 °C again. As the melt of **1** would flow down along the quartz plate, we were unable to measure the accurate emission intensity of **DETPS** in the melt state of **1**. Herein we monitor the change of the emission intensity of the mixture with **1** in the Cr phase at RT to check the reproducible ability.  $\lambda_{\text{ex}} = 380 \text{ nm}$ . We have also measured the emission intensity of **DETPS** in the **1** matrix with the  $\text{LC}_x$  phase in the same way, and found the emission intensity almost unchanged after 4 repeating cycles.

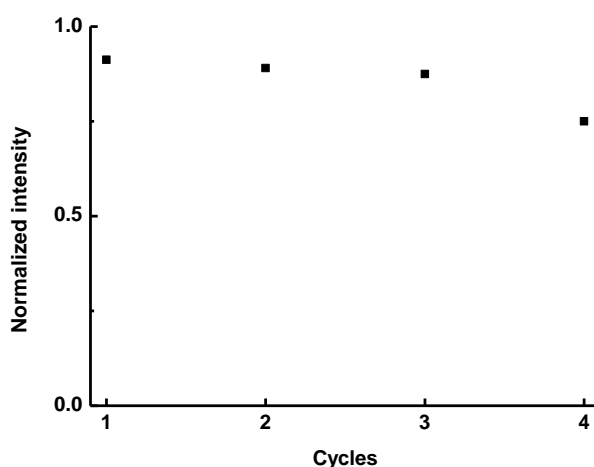


**Figure S23.** Fluorescent intensities at 500 nm of the shear-induced phase measured from the four repeating cycles mentioned in Figure S21.

## References

- [1] J. W. Chen, C. C. W. Law, J. W. Y. Lam, Y. P. Dong, S. M. F. Lo, I. D. Williams, D. B. Zhu, B. Z. Tang, *Chem. Mater.* **2003**, *15*, 1535.
- [2] Xu, J. W.; Lai, Y. H.; He, C. B. *Org. Lett.* **2002**, *4*, 3911.
- [3] Percec, V.; Ahn, C. H.; Bera, T. K.; Ungar, G.; Yeardley, D. J. P. *Chem. Eur. J.* **1999**, *5*, 1070.
- [4] B. Y. Tang, J. J. Ge, A. Q. Zhang, B. Calhoun, P. W. Chu, H. B. Wang, Z. H. Shen, F. W. Harris, S. Z. D. Cheng, *Chem. Mater.* **2001**, *13*, 78.

- [5] a) V. S. K. Balagurusamy, G. Ungar, V. Percec, G. Johansson, *J. Am. Chem. Soc.* **1997**, *119*, 1539;  
b) V. Percec, W. D. Cho, G. Ungar, D. J. P. Yeardley, *J. Am. Chem. Soc.* **2001**, *123*, 1302.  
[6] T. Iwaki, C. Torigoe, M. Noji and M. Nakanishi, *Biochemistry*, **1993**, *32*, 7589.